Construction of a Dynamic Evaluation System for Cross-Platform Social Media Marketing Effectiveness Integrating Federated Learning

Shihua Zuo
Department of Economics and Trade, Hunan Mechanical and Electrical Polytechnic, Changsha 410151, Hunan, China
Corresponding author: Shihua Zuo (e-mail: zuoshihua2005@126.com)

ABSTRACT Existing cross-platform social media marketing evaluation methods are vulnerable to selection bias, attribution error, and privacy risk, which restricts dynamic evaluation accuracy. This paper develops a privacy-preserving dynamic evaluation system for cross-platform social media marketing effectiveness based on federated learning. The system integrates advertisers as label holders and social platforms as feature providers, and applies private set intersection with hash encryption for secure user alignment. A vertical federated neural network combining secure multi-party computation and differential privacy is then used to aggregate hidden-layer outputs securely. A federated causal attribution mechanism based on Shapley values and counterfactual prediction dynamically quantifies the marginal contribution of each platform to conversion. The experimental data cover user behavior logs from Douyin, Weibo, and Xiaohongshu from January to December 2023, involving 40,000 cross-platform users and 5,862 conversion events, supplemented by a public digital marketing dataset for generalization validation. The proposed model achieves an AUC of 0.897 and attribution consistency of 0.766, outperforming FedAvg, FedTime, and FedDP by up to 46.5%. The information leakage risk probability is reduced to 0.184. These results demonstrate that the system improves the accuracy, interpretability, and privacy protection of cross-platform marketing evaluation.

INDEX TERMS cross-platform social media, marketing evaluation, federated learning, causal attribution, privacy protection

I. INTRODUCTION

AMID the rapid development of social media, cross-platform marketing has become a crucial means for companies to achieve brand communication and targeted reach—a necessity acutely felt by the industry as it seeks to weave its products into the global digital marketplace. In the real world of simultaneous multi-platform marketing, dynamic evaluation of new media marketing effectiveness remains challenging. Inconsistent data standards and statistical calibers across platforms introduce biases and distortions in cross-platform integration. These discrepancies make it difficult to align the behavioral trajectories of the same user across different platforms, which can seriously mislead budget allocation decisions [1,2]. At the same time, due to data protection restrictions and platform technical barriers, original user behavior data is difficult to share across platforms, resulting in the formation of data islands. As a result, existing methods rely more on local sampling or centralized aggregation, which not only sacrifices evaluation integrity but also faces compliance risks [3,4]. Most existing attribution analysis methods are based on behavioral records from a single platform, lacking a cross-platform research perspective and making it difficult to comprehensively capture the entire user interaction and conversion process. Furthermore, without randomized controls, the ability to identify causal effects is weak, and dynamic effect evaluations suffer from significant biases, resulting in a lack of scientific basis for marketing resource allocation and optimization [5,6]. How to conduct high-precision collaboration and dynamic effect evaluation of cross-platform data while ensuring privacy and security is a key issue that urgently needs to be addressed in new media marketing.

Current research focuses on breaking the limitations of single-platform data and building a quantifiable and comparable cross-platform marketing performance evaluation system [7,8]. It mainly develops along three technical paths. The first type of method focuses on multi-channel data integration. To comprehensively evaluate cross-platform marketing performance, Kufile Omolola Temitope proposed a unified attribution model suitable for dynamic, multi-channel environments, emphasizing the impact of data granularity and real-time processing on model construction. This provides a theoretically rigorous and practically feasible roadmap for cross-channel marketing performance evaluation and promotes the development of attribution science in the digital environment [9]. The second type of method focuses on cross-platform market structure and behavior analysis. In response to the limitations of single-platform data, Kou Gang proposed a cross-platform marketing structure analysis method based on multi-attribute group decision-making. By building a cross-platform analysis framework, online reviews from multiple e-commerce platforms were integrated. The results showed that this method could effectively identify market structure characteristics and provide data support for enterprises to optimize product design and competitive strategies [10]. To guide product launch and distribution strategies, Krijestorac Haris used the dissemination data of 381 videos on 26 platforms to construct a synthetic control model to evaluate the reverse spillover marketing effect, providing an important basis for content distribution strategy and platform ecosystem management [11]. The third type of method attempts a data-driven unified analysis framework. Poturak Mersid further constructed a unified analysis framework that integrated population, platform, and participation, revealing the key role of precise audience targeting and channel optimization in improving advertising marketing, and providing empirical evidence and practical guidance for digital marketing strategies [12]. Kaveh Mojtaba used system dynamics and network data envelopment analysis tools to simulate causal loop diagrams and traffic inventory diagrams, and used the simulation results as input to the data envelopment analysis model to achieve effective analysis of marketing performance [13]. To address data silos and privacy constraints, research in recent years has shifted to distributed collaborative modeling based on federated learning (FL), focusing on achieving cross-platform intelligent decision-making without sharing original data [14,15]. Zhang Kai proposed a privacy-preserving FL framework for digital marketing scenarios, integrating differential privacy (DP) and homomorphic encryption technology, and optimizing cross-platform performance through an adaptive model aggregation strategy with dynamic weight adjustment. Verification based on ultra-large-scale real data showed that the framework significantly improved advertising effectiveness while protecting privacy [16]. In response to the problem of data silos restricting open innovation, Zhang Xiaodong proposed an intelligent decision-making model based on FL, which achieved distributed collaborative learning while ensuring the privacy and security of enterprise data at each node. By comparing the prediction effects of overall learning, local learning, and FL, the latter's advantage in improving prediction accuracy was verified [17]. Kim Dohyoung classified and reviewed existing FL methods from the dimensions of data partitioning, privacy mechanisms, model architecture, etc., emphasizing that it can promote fair model training and enhance privacy protection in a cross-platform distributed environment [18]. To address these challenges, this article investigates a cross-platform dynamic social media marketing effectiveness evaluation system integrated with FL. The innovations of this article are:

(1) To address the challenge of data non-shareability, a private set intersection (PSI) method based on hash encryption and Bloom filters is used to securely align users across platforms. This method achieves encrypted alignment of user identities and collaborative construction of feature spaces without exposing non-overlapping users.

(2) To address issues of static evaluation and high attribution bias, a streaming dynamic modeling architecture based on vertical federated learning (VFL) is designed, combined with Apache Flink for real-time feature updates and model inference, overcoming the limitations of traditional post-evaluation.

(3) To address the vulnerability of fragile causal identification, a federated attribution algorithm based on Shapley values is applied to quantify the marginal contribution of each platform through counterfactual predictions, improving attribution interpretability and the value of marketing decisions.

This article offers companies an actionable decision-making basis for cross-platform advertising budget allocation and channel optimization, providing a vital reference for the sustainable development of the marketing technology ecosystem in privacy-compliant environments—a transparency requirement parallel to the ethical and traceable supply chains increasingly demanded within the industry.

II. CONSTRUCTION OF A DYNAMIC EVALUATION SYSTEM FOR CROSS-PLATFORM SOCIAL MEDIA MARKETING EFFECTIVENESS

The architecture of the dynamic evaluation system for cross-platform social media marketing effectiveness integrated with FL, as constructed in this article, is shown in Figure 1:

As shown in Figure 1, the system adopts a four-layer collaborative architecture, encompassing the data collaboration layer, federated modeling layer, dynamic evaluation layer, and decision feedback layer. The system first implements privacy-preserving alignment of cross-platform user identities in the data collaboration layer. Using PSI technology based on hash encryption and Bloom filters, it identifies co-occurring user groups across multiple platforms without revealing the identities of non-overlapping users. Under the leadership of the label provider, a shared label alignment mechanism required by VFL is constructed. User behavior features are extracted locally on each platform to form a heterogeneous yet aligned joint feature space, ensuring data availability without visibility.

At the federated modeling layer, the system deploys a vertical federated neural network model. Each participating platform performs forward computation and gradient generation based on a local feature subset. Intermediate variables

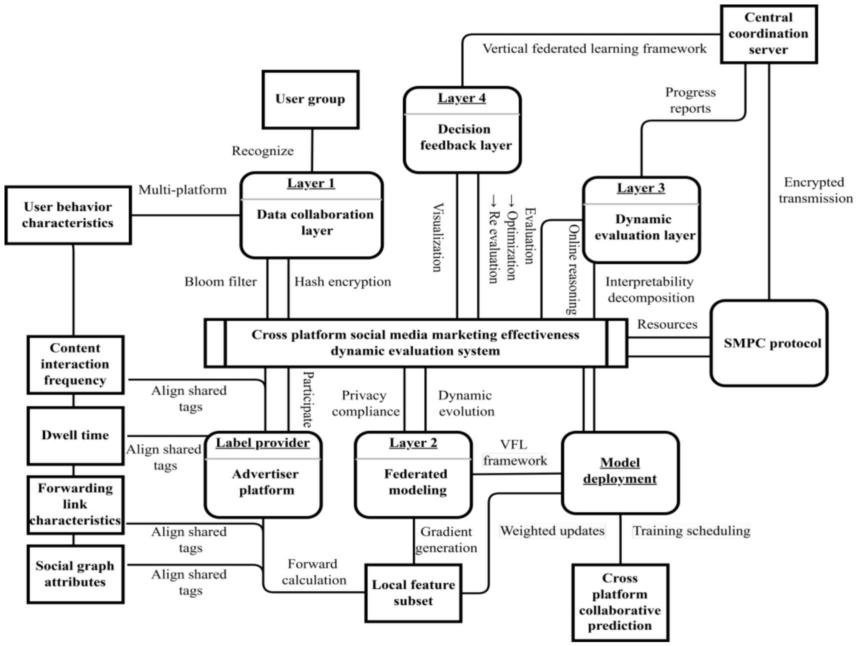

FIGURE 1. Dynamic evaluation system architecture for cross-platform social media marketing effectiveness

are encrypted and transmitted to a central coordination server via the secure multi-party computation (SMPC) protocol. The server aggregates the model and issues updated parameters. This layer combines DP and gradient clipping to prevent information leakage and supports periodic and incrementally triggered collaborative training, ensuring dynamic model evolution and privacy compliance. To more clearly illustrate the specific implementation sequence of privacy protection mechanisms in the modeling process, Figure 2 further details the steps from user alignment to model training, including the synergistic effects of PSI, VFL, SMPC, and DP:

PSI is used to align user identities across multiple platforms without revealing the identities of users from non-intersecting sets; SMPC is used to encrypt and aggregate intermediate computation results from all participants; DP prevents model updates from leaking individual information by injecting controllable noise into gradients; VFL is suitable for scenarios where all parties hold the same samples but have different feature dimensions, and is the core framework for collaborative modeling in this system.

The dynamic evaluation layer leverages Apache Flink to build a streaming data processing pipeline. Behavior logs reported in real time by various platforms are cleaned, windowed, and feature-engineered to generate standardized input vectors. Trained federated models are then invoked for online inference, outputting dynamic evaluation results such as user conversion probability and influence scores. Federated Shapley Additive Explanations (SHAP) is also integrated to enable interpretable decomposition of cross-platform contribution metrics.

At the decision feedback layer, the system presents performance data charts, return on investment (ROI) trend analysis, and user journey paths for each platform through a visualization platform. It also utilizes reinforcement learning to generate budget optimization recommendations, which are fed back to each platform's delivery system via an interface, enabling a seamless transition from evaluation to optimization to re-evaluation.

III. ENCRYPTED ALIGNMENT OF MULTI-PLATFORM USER IDENTIFIERS AND COLLABORATIVE FEATURE SPACE CONSTRUCTION

To break down data silos, this article utilizes PSI technology based on hash encryption and Bloom filters. Using TikTok, Weibo, and Rednote as participating social media platforms (Platform A, Platform B, and Platform C), user account IDs (identifiers) across each platform are securely matched to identify co-occurring user sets across platforms without exposing non-overlapping user information. Led by the label provider, the shared label alignment mechanism required by VFL is established. Each platform extracts user behavior features locally, forming heterogeneous feature subsets belonging to different platforms but based on the same user population, which form the basis of a joint feature space.

Suppose the platform set is $P = \{A, B, C\}$, each platform has a local user ID set $U_P = \{id_{P,1}, id_{P,2}, \cdots, id_{P,n_P}\}$. To avoid direct exchange of original IDs, each platform uses a consistent, pre-agreed keyed hash map $h_K(\cdot)$:

$$\widetilde{id}_{P,i} = h_K(id_{P,i}) \in \{0,1\}^L \tag{1}$$

where, L is the hash output bit length, and K is the session key. The hash map ensures the difficulty of reversing the original identity and meets the basic irreversibility requirement. Each platform inserts the hash value set into the

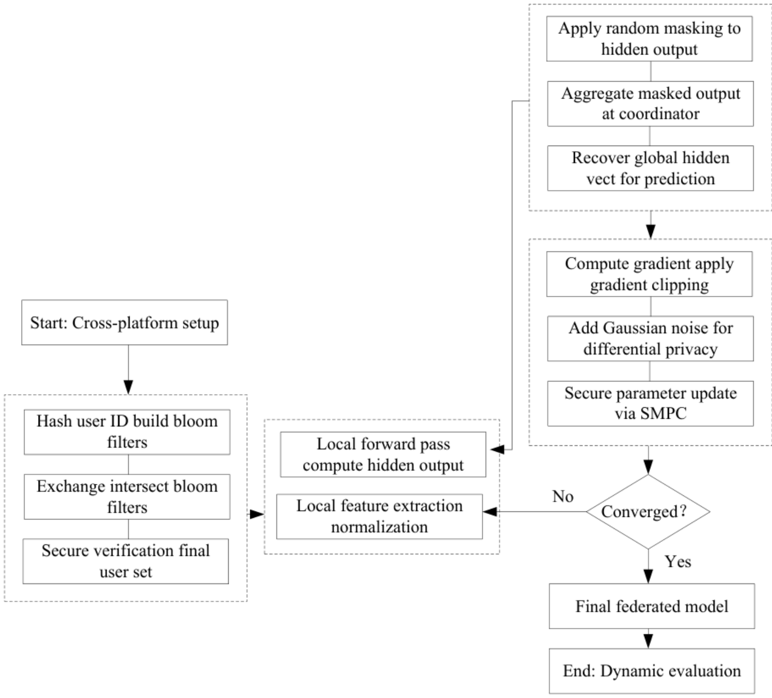

FIGURE 2. Privacy collaborative modeling process

local Bloom filter BF_P, whose bit length is m, and the hash function group is $H = \{h_1, \cdots, h_k\}$. The insertion rule is to calculate k Bloom hashes for each $\widetilde{id}$ and set them. The Bloom filter allows efficient set operations and transmission, and its false positive, no false negative characteristics can control its error rate p_{fp} through m, k, which is expressed as [19]:

$$p_{\text{fp}} \approx (1 - e^{-kn/m})^k \tag{2}$$

where, n is the number of inserted elements. To minimize p_{fp}, the optimal hash number is selected [20,21]:

$$k^* = \frac{m}{n} \ln 2 \tag{3}$$

Based on this, the required bit length m is reversely determined to meet the given p_{fp}. After the Bloom filter is constructed, the platforms exchange their respective BF_P and perform a bitwise AND operation on the bit vectors in the encrypted domain to obtain the candidate intersection Bloom filter:

$$BF_\cap = \bigwedge_{p \in P} BF_P \tag{4}$$

Due to the existence of false positives in the Bloom filter, the intersection bit vector only locates the candidate set. To eliminate false positives and obtain the precise co-occurring user set $U_\cap$, the system performs a second-stage verification on the candidate set: each participant calculates a salted signature s_p for its candidate ID and only submits the encrypted summary of the candidate signature to the coordinator. The coordinator completes the equality judgment under the ciphertext protocol to confirm the final intersection $U_\cap$.

After completing user alignment, collaborative construction of the feature space begins. For the intersection user set $U_\cap = \{u_1, u_2, \cdots, u_N\}$, each platform extracts the native behavior feature vector $x_P(u) \in \mathbb{R}^{d_P}$ for each user u locally, including content interaction frequency, dwell time, forwarding link characteristics, and social graph attributes. The platform's total feature matrix is recorded as $X_P \in \mathbb{R}^{N \times d_P}$. To ensure the comparability of features across platforms on a statistical scale, each platform performs a local normalization transformation:

$$\overline{x}_P(u) = \frac{x_P(u) - \mu_P}{\sigma_P} \tag{5}$$

where, μ_P and σ_P are the local mean and standard deviation of the corresponding features of the platform, which are only calculated locally and not leaked externally. The normalized local features constitute the input of the VFL.

In real-world cross-platform marketing data, issues such as user ID noise, incompleteness, or slight mismatches are common, potentially affecting the recall rate of PSI alignment. To address this, this article introduces a lightweight preprocessing mechanism before PSI: First, each platform performs standardization and cleaning on the original IDs; then, multiple ID variants suspected to belong to the same user are clustered and merged locally to generate a unified anonymous identifier (UID) within the platform. This process is completed locally and does not involve cross-platform information exchange. Based on this, PSI performs intersection calculations using the standardized UIDs, reducing the risk of missed alignment due to ID heterogeneity. If the PSI recall rate is too low, the system will trigger a feature imputation strategy to mitigate sample bias and ensure model training stability.

IV. COLLABORATIVE TRAINING OF DYNAMIC EVALUATION MODELS BASED ON VFL

A privacy-preserving collaborative training mechanism is constructed based on the encrypted alignment of multi-platform user identifiers and the construction of a joint feature space, a privacy-preserving collaborative training mechanism for cross-platform marketing effectiveness evaluation models. While maintaining the original data strictly locally and preventing cross-platform transmission, co-occurring user conversion behaviors are jointly modeled, and a dynamic evaluation model that supports the capture of nonlinear relationships is constructed. The system utilizes the VFL framework, as shown in Figure 3, with advertisers as label providers and social media platforms as feature providers, jointly training the model. During training, encrypted aggregation, SMPC, and DP are used to ensure that intermediate information cannot be reversed back to the original data from a single party. Training scheduling and weighted update strategies address platform heterogeneity and sample imbalance, enabling cross-platform collaborative prediction.

In the VFL framework, the goal is to learn the joint mapping $f : X_A \times X_B \times X_C \to Y$. Each platform defines a differentiable feature transformer $g_P(\cdot; \theta_P)$ locally, whose output is a local latent representation:

$$z_P(u) = g_P(\overline{x}_P(u); \theta_P) \tag{6}$$

The label provider holds the corresponding label set $Y = \{y(u)\}_{u \in U_\cap}$. The global prediction structure adopts the form of concatenating the latent representations at the coordinator and generating predictions by global parameters ω, b:

$$Z(u) = \sum_{p \in P} z_p(u) \tag{7}$$

$$\hat{y}(u) = \delta\left(\omega^\top [z_A(u); z_B(u); z_C(u) + b]\right) \tag{8}$$

where, $[\cdot;\cdot]$ represents vector concatenation; δ is the activation function sigmoid; ω, b are global trainable parameters. The loss function is binary cross-entropy:

$$L = \frac{1}{N} \sum_{u \in U_\cap} [-y(u) \log \hat{y}(u) - (1 - y(u)) \log(1 - \hat{y}(u))] \tag{9}$$

Parameter updates follow the backpropagation chain. The coordinator calculates the gradient $\partial L / \partial z_P$ with respect to the aggregate representation and distributes the gradient back to each platform in the form of secret sharing. Each platform obtains the gradient of its parameters based on the chain derivation of the local model [22,23]:

$$\frac{\partial L}{\partial \theta_P} = \sum_{u \in U_\cap} \left(\frac{\partial L}{\partial Z(u)}\right)^\top \frac{\partial z_P(u)}{\partial \theta_P} \tag{10}$$

The parameter update $\theta_P \leftarrow \theta_P - \eta_P \partial L / \partial \theta_P$ is completed locally. The coordinator also updates the global trainable parameters ω, b. During model training, for each round of communication, each $u \in U_\cap$, platform P locally calculates its latent representation $z_P(u)$. To prevent the leakage of unilateral representation, the platform generates a random mask vector $s_P(u)$ that satisfies the secret sharing construction of $\sum_P s_P(u) = 0$ and sends the masked representation [24]:

$$\widetilde{z}_P(u) = z_P(u) + s_P(u) \tag{11}$$

The coordinator performs vector summation on the received $\widetilde{z}_P(u)$:

$$\widetilde{Z}(u) = \sum_P \widetilde{z}_P(u) = \sum_P z_P(u) + \sum_P s_P(u) = Z(u) \tag{12}$$

Since the random masks added locally cancel each other out during global aggregation, the coordinator can only recover the true aggregation result Z(u), but cannot disassemble the individual contribution of any participant, ensuring privacy security at the implicit representation level [25,26].

The label holder calculates the predicted $\hat{y}(u)$ and sample loss $l(\hat{y}, y)$ based on $Z(u)$ and label $y(u)$, and then obtains the gradient with respect to $Z(u)$:

$$\frac{\partial L}{\partial Z(u)} = (\hat{y}(u) - y(u))\omega \tag{13}$$

The coordinator returns $\partial L / \partial Z(u)$ to each platform in the form of secret sharing, and each platform performs gradient clipping after receiving it locally [27]:

$$\overline{g}_P = \frac{g_P}{\max(1, \|g_P\|_2 / c)} \tag{14}$$

Gaussian noise is then added to achieve DP:

$$\widetilde{g}_P = \overline{g}_P + \mathcal{N}(0, T^2 c^2 I) \tag{15}$$

The noise scale T is configured by the target (ϵ,ϕ) budget. c is the sensitivity. After the local parameters are updated, the platform submits the necessary update summaries in encrypted or secret-shared form, and the coordinator updates ω, b based on this information [28,29]:

$$\omega \leftarrow \omega - \eta_\omega \frac{1}{N} \sum_u \frac{\partial l}{\partial Z(u)} \cdot Z(u)^T \tag{16}$$

$$b \leftarrow b - \eta_\omega \frac{1}{N} \sum_u \frac{\partial l}{\partial Z(u)} \cdot Z(u) \tag{17}$$

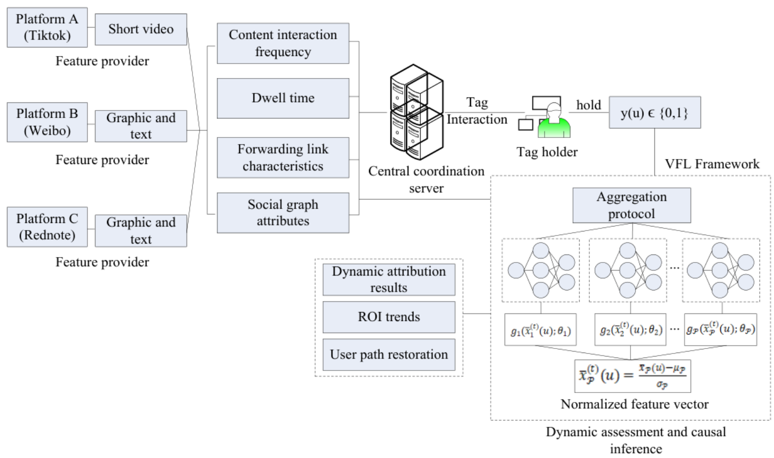

FIGURE 3. VFL framework and collaborative training

The above updates are completed in the ciphertext domain to ensure that a single party cannot infer the other party's representation through intermediate quantities. Training is iterated in rounds of $t = 1, \cdots, T$, and the system is triggered based on the data increment threshold $\Delta D_P^{(t)} = \|x_P^{(t)} - x_P^{(t-1)}\|_F / \|x_P^{(t-1)}\|_F > \varsigma$. In SMPC, each party P generates a random vector fragment $r_{P,q}(u)$ for each u_i and sends it to other participants Q_q, respectively, so that:

$$s_P(u) = \sum_{q \neq P} r_{P,q}(u) - \sum_{q \neq P} r_{q,P}(u) \tag{18}$$

To achieve the desired goal (ϵ,ϕ), the single release condition of the Gaussian mechanism is adopted: when the sensitivity is c, the noise standard deviation is assumed to satisfy:

$$T \geq \frac{c\sqrt{2\ln(1.25/\phi)}}{\epsilon} \tag{19}$$

Then, the single report satisfies (ϵ,ϕ). The total privacy loss of multiple rounds of training is accumulated and calculated by the advanced composition theorem, thereby adjusting the rounds. The risk of implicit representation inversion attack decreases as the noise variance increases; gradient clipping limits the sensitivity of a single sample to c, and combined with masking and SMPC, the probability of single-party inversion is reduced to a negligible level. To avoid the long-term cumulative risk of sample leakage, the system periodically resets the session key K and mask generation seed during long-term operation. To alleviate the imbalance of sample size and feature dimension between platforms, an adaptive local learning rate is adopted:

$$\eta_{\mathrm{P}} = \eta \cdot \alpha_{\mathrm{P}} \tag{20}$$

The weight is $\alpha_{\mathrm{P}} = \sqrt{N_{\mathrm{P}}} / \sum_q \sqrt{N_q}$, and N_{P} is the number of intersection samples of platform P. A weighted update with regularization is performed on the coordinator side to suppress the noise amplification effect of small-sample parties. The gradient clipping, DP noise, and communication overhead of each round in model training are shown in Figure 4:

Figure 4 illustrates the privacy protection mechanism and communication efficiency control of VFL in practical applications. Figure 4A shows the evolution of gradients from original gradients to clipped gradients and then to noisy gradients. Clipping limits the upper limit of a single user's contribution to the overall model, preventing extreme values from leaking feature information. Gaussian noise perturbation ensures that user data meets the (ϵ,ϕ) constraint when uploaded, thus achieving a balance between availability and privacy. In Figure 4B, after implementing secure aggregation and gradient compression mechanisms, the per-round communication cost of each platform remains within a relatively controllable range.

V. DYNAMIC EFFECT ESTIMATION AND CAUSAL INFERENCE

User behavior data collected from various social media platforms is converted into standardized feature vectors that can be inferred online. Based on the trained VFL model, cross-platform user conversion probabilities and marketing influence indices are dynamically calculated to achieve real-time effect evaluation. Finally, through federated attribution and causal inference analysis, the contribution of each platform to the overall marketing effect is decomposed; causal relationships are identified; and precision marketing strategy optimization is supported. The dynamic evaluation in this paper is mainly achieved through a two-layer update mechanism:

(1) Model level: The federated model adopts an incremental, trigger-based retraining strategy, performing a complete collaborative training every 24 hours. Simultaneously, when the amount of new behavior logs from any platform exceeds a preset threshold, an asynchronous local update is triggered

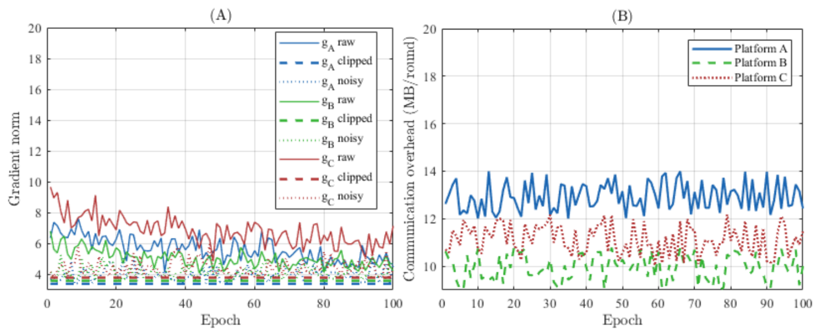

FIGURE 4. Privacy protection and communication efficiency mechanism. Figure 4A: Gradient clipping and DP noise; Figure 4B: Per-round communication cost

to ensure the model captures user behavior drift in a timely manner.

(2) Attribution and inference level: A streaming pipeline built on Apache Flink continuously aggregates real-time user behavior using a sliding time window (window size = 1 hour, sliding step = 15 minutes), generates standardized feature vectors, and calls the latest federated model for online inference. The attribution module synchronously calculates Shapley values according to the window, forming a time series of platform contributions.

First, the real-time behavior log stream $S_P = \{(u, t, e_P)\}$ is received through the API provided by each platform. e_P represents the event that occurred to user u on platform P at time t. The log stream is processed by Apache Flink to build a streaming feature engineering pipeline based on a time sliding window. Assuming that the window size is $\Delta T = 5$ min, and the sliding step size is $\xi_T = 1$ min, for each user u, the behavior features $x_P^{(t)}(u) = [f_{\text{click}}^{(W_t)}, t_{\text{dwell}}^{(W_t)}, d_{\text{share}}^{(W_t)}, \rho_{\text{fan}}]$ are aggregated in the current window W_t. f_{click} is the click frequency; t_{dwell} is the average dwell time; d_{share} is the forwarding link depth; ρ_{fan} is the static social graph attribute vector. Subsequently, each platform uses the local normalization parameter (μ_P, σ_P) to normalize the features:

$$\overline{x}_P^{(t)}(u) = \frac{\overline{x}_P(u) - \mu_P}{\sigma_P} \tag{21}$$

A standardized input vector is generated. This vector is input into the locally deployed federated model, and forward propagation is performed to calculate the local hidden representation:

$$z_P^{(t)}(u) = g_P(\overline{x}_P^{(t)}(u); \theta_P) \tag{22}$$

Following the aggregation protocol, $\overline{z}_P^{(t)}(u)$ is uploaded to the coordination server through the SMPC and masking mechanism. Without decrypting the unilateral representation, the coordinator reconstructs the aggregated latent vector $Z^{(t)}(u)$:

$$Z^{(t)}(u) = \sum_{p \in P} \overline{z}_P^{(t)}(u) \tag{23}$$

The final prediction score is calculated as follows:

$$\hat{y}^{(t)}(u) = \delta\left(\omega^\top [z_A^{(t)}(u); z_B^{(t)}(u); z_C^{(t)}(u) + b]\right) \tag{24}$$

To further realize the causal level of platform contribution attribution, the system applies the Shapley value decomposition mechanism in the federated environment. In the platform set $P = \{A, B, C\}$, the feature contribution function $v(S)$ is defined as the expected conversion probability predicted by using only the features of the subset $S \subseteq P$:

$$v(S) = E_{u \sim D}[\delta(\omega_S^\top Z_S(u) + b)] \tag{25}$$

The Shapley value of platform P is defined as [30,31]:

$$\phi_P = \sum_{S \subseteq P \setminus \{p\}} \frac{|S|!(|P| - |S| - 1)!}{|P|!}[x(S \cup \{p\}) - v(S)] \tag{26}$$

where, ϕ_P represents the weighted average of the marginal performance improvement brought by platform P in all possible feature combinations. Given that accurately calculating the Shapley value requires traversing all combinations of platform subsets, its time complexity is $O(2^M)$ (where M is the number of participating platforms), which is an NP-hard problem in cross-platform scenarios. This article adopts an approximate Shapley value algorithm based on Monte Carlo sampling [32]:

$$\hat{\phi}_P = \frac{1}{M} \sum_{m=1}^{M} [\hat{y}(Z_{S_m \cup \{p\}}) - \hat{y}(Z_{S_m})] \tag{27}$$

The system sets the number of samples K to 500, reducing the complexity to $O(KM)$, where S_m is a randomly sampled feature subset. This calculation is completed on the coordinator side based on the aggregated latent vector, without accessing the original features of any unilateral party, thereby meeting the privacy constraint. To support dynamic attribution, the system continuously calculates $\hat{\phi}_P^{(t)}$ in a sliding window to form a time series $\Phi_P = \{\hat{\phi}_P^{(t)}\}_{t=1}^{T}$ for analyzing the contribution evolution of each platform in different marketing stages. The attribution results are weighted and smoothed [33,34]:

$$\widetilde{\phi}_P^{(t)} = \alpha \widetilde{\phi}_P^{(t-1)} + (1-\alpha)\hat{\phi}_P^{(t)} \tag{28}$$

In the decision feedback layer, the high-dimensional, time-varying federated evaluation results are converted into a visualization view to assist operators in understanding the cross-platform synergy effect. Based on the dynamic attribution results and ROI trends, intelligent budget reallocation decisions are made.

In the platform contribution visualization, the intensity of the normalized $\widetilde{\phi}_P^{(t)}$ is mapped to reveal the evolution of the relative influence of each platform in different time periods. The user path restoration graph reconstructs the typical conversion path based on the Markov chain model and calculates the state transition probability from platform i to platform j [35,36]:

$$P_{ij} = \frac{N_{i\to j}}{\sum_{k\in P} N_{i\to k}} \tag{29}$$

where, $N_{i\to j}$ is the frequency of the user's next contact point being j after contacting platform i, which is used to identify high-frequency communication links. The ROI dynamic curve calculates the input-output ratio of each platform at the hourly granularity:

$$ROI_P^{(t)} = \frac{\sum_{u\in U_P^{(t)}} \hat{y}^{(t)}(u)\cdot \text{value}}{\text{cost}_P^{(t)}} \tag{30}$$

where, value is the average customer unit price, and $\text{cost}_P^{(t)}$ is the advertising expenditure of platform P in time window t, which is used to guide budget allocation.

VI. PERFORMANCE VERIFICATION OF THE DYNAMIC EVALUATION SYSTEM FOR CROSS-PLATFORM SOCIAL MEDIA MARKETING EFFECTIVENESS

A. EXPERIMENTAL DATA

The experimental data sources for this article consist of two main components: the first is the actual marketing data from three mainstream social media platforms (Platform A: TikTok, Platform B: Weibo, and

Platform C: Rednote); the second is the publicly available digital_marketing_campaign_dataset, which supplements comparative experiments and validation in cross-platform marketing scenarios. By combining real platform data with publicly available datasets, the system's validation is broad and reproducible. For Platform A (TikTok), video behavior data is extracted from a brand's advertising campaign on TikTok, with a sample size limited to 125,031 behavior logs corresponding to 20,000 users. For Platform B (Weibo), a sample of brand topic promotion on Weibo is selected, encompassing 15,000 users and 98,366 interaction records. For Platform C (Rednote), a community note promotion sample is used, sampling approximately 5,000 users and 22,014 note-related interaction records. In the public dataset section, this article uses the digital_marketing_campaign_dataset from Kaggle. This dataset contains advertising and social media interactions from multiple digital marketing campaigns, including 5,000 users and their behavior records. Table 1 shows the basic experimental data information:

The VFL model constructed in this article uses neural networks in local nodes on each platform, with a central coordinator performing weighted aggregation. The core parameter configuration is shown in Table 2.

To comprehensively evaluate system performance, validations are conducted from the perspectives of marketing effectiveness evaluation, causal effect identification, marketing optimization, and privacy protection and compliance, and the following comparison methods are set:

(1) FedAvg: Each platform independently trains the model locally and then performs a global update through weighted averaging, without considering feature heterogeneity or cross-platform causal relationships.

(2) FedTime: Based on FedAvg, it adds time series feature input of user behavior but still does not model causal effects.

(3) FedDP: Based on FedAvg, it adds gradient clipping and DP noise to achieve user privacy protection.

This article aims to achieve cross-platform causal attribution under privacy constraints. Current mainstream causal attribution methods, such as the Shapley Attribution Model, rely on centralized user behavior sequences and cannot be directly applied to federated environments. To maintain the fairness and feasibility of the experiment, this article selects three widely used benchmark models in federated environments—FedAvg, FedTime, and FedDP—as controls to examine the incremental improvement of the proposed federated causal attribution framework in causal consistency metrics under the same privacy protection conditions.

VII. EXPERIMENTAL RESULTS

A. MARKETING EFFECTIVENESS EVALUATION

To verify the effectiveness of the system constructed in this article, the accuracy and stability of the model in cross-platform conversion prediction tasks are analyzed in the dimension of marketing effectiveness evaluation. Logarithmic loss is used to measure the calibration of the model's predicted probabilities, while prediction accuracy is used to evaluate overall classification performance. The performance of the proposed model compared to the comparison models on the same test set is shown in Figure 5:

In Figure 5, the proposed model outperforms the three comparison models—FedAvg, FedTime, and FedDP—in both logarithmic loss and accuracy. This demonstrates that the proposed model is able to more effectively integrate cross-platform user data while preserving the privacy of local features, thereby achieving more precise cross-platform marketing effect predictions. Figure 5A shows that the logarithmic loss of each model decreases with each training epoch, indicating that the training process is gradually converging. The proposed model converges quickly and achieves the lowest final loss. In Figure 5B, the proposed model achieves the highest accuracy of 0.876, surpassing

TABLE 1. Basic experimental data information

Platform/Dataset	Data Type	Number of Users	Time Span	Key Features
TikTok	Video interaction data	20,000	01/2023–12/2023	Views, likes, comments, reposts, follower conversions
Weibo	Topic and blog post data	15,000	01/2023–12/2023	Views, reposts, comments, topic popularity, user tags
Rednote	Note interaction data	5,000	01/2023–12/2023	Exposure, likes, engagement rate
digital_marketing_campaign_dataset	Advertising and social media marketing campaign data	5,000	Multi-platform, multi-year	Conversion rate (CVR), click-through rate (CTR), website visits, social shares

TABLE 2. Model parameter configuration

Classification	Parameter	Specification
Training Configuration	Local batch size	128
Training Configuration	Learning rate	0.001 (Adam optimizer)
Training Configuration	Hidden layer dimensions	128, 64
Training Configuration	Communication frequency	Once every 24 hours
Training Configuration	Number of local training epochs	5 local iterations before each communication round
Privacy Protection Mechanism	Gradient clipping threshold	1
Privacy Protection Mechanism	Noise standard deviation	1.2
Privacy Protection Mechanism	Security protocol	SMPC + secret sharing

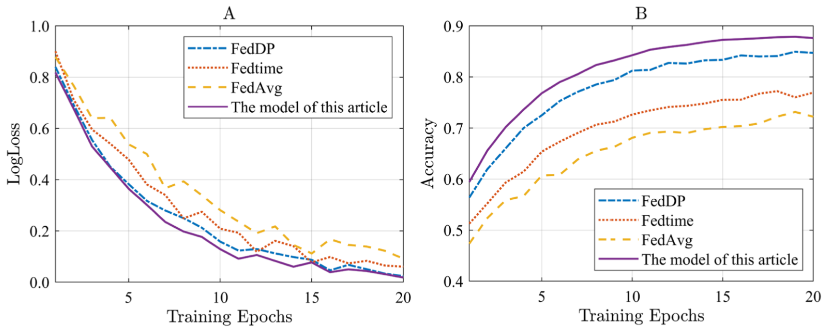

FIGURE 5. Logarithmic loss and accuracy. Figure 5A: Logarithmic loss results; Figure 5B: Accuracy results

all other models. Overall, the proposed model is able to fully utilize heterogeneous cross-platform information while ensuring data privacy, demonstrating its ideality and applicability. FedTime and FedAvg, as conventional FL methods, achieve basic performance but fail to consider dynamic causality and feature heterogeneity. While FedDP enhances privacy protection, it sacrifices performance.

In cross-platform marketing effectiveness evaluation, user conversion prediction is a core task in measuring the effectiveness of marketing strategies. To comprehensively evaluate the model's discriminative ability across different social media platforms, this article uses AUC as an evaluation metric. This reflects the model's ability to distinguish between converting and non-converting users at various decision thresholds and measures the impact of cross-platform feature heterogeneity on prediction performance. The results are shown in Figure 6.

In Figure 6, the proposed model demonstrates a significant advantage in capturing user behavior patterns and predicting conversions. In Figure 6A, the proposed model achieves the highest AUC value, reaching 0.897, demonstrating its strong ability to distinguish between converting and non-converting users. It fully captures cross-platform feature heterogeneity and dynamic behavior patterns, enabling more precise marketing effectiveness evaluation. The FedDP model in Figure 6B performs second, with an AUC of 0.862, slightly lower than the proposed model. While the application of DP noise protects data privacy, it also reduces prediction accuracy. FedTime in Figure 6C further degrades, achieving an AUC of 0.784. This is due to its simple averaging strategy, which ignores feature differences and platform bias, limiting its predictive power. The FedAvg model in Figure 6D performs the worst, with an AUC of 0.761. While it has some advantages in processing time series features, it is prone to information loss when integrating heterogeneous data from multiple platforms, resulting in a reduced ability to distinguish between positive and negative samples.

B. CAUSAL EFFECT IDENTIFICATION

To verify the accuracy of the proposed model in identifying causal effects in cross-platform marketing scenarios, attribution consistency and platform blocking prediction error are used as evaluation metrics. The former measures the consistency between Shapley attribution results and counterfactual effects, comparing the model's Shapley attribution output for each platform with the change in counterfactual conversion probabilities constructed based on real intervention data. The latter evaluates the system's sensitivity to platform loss, simulating the prediction error in user conversion probabilities after closing platform touchpoints to measure the model's causal sensitivity to missing platform behavior. The comparison results are shown in Figure 7:

In Figure 7, compared with the comparison models, the

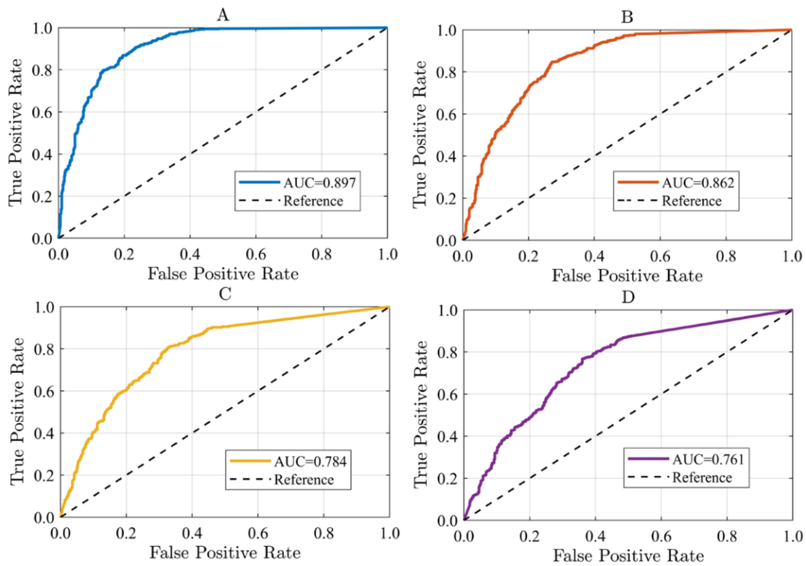

FIGURE 6. User conversion prediction AUC values. Figure 6A: AUC values of the proposed model; Figure 6B: AUC values of FedDP; Figure 6C: AUC values of FedTime; Figure 6D: AUC values of FedAvg

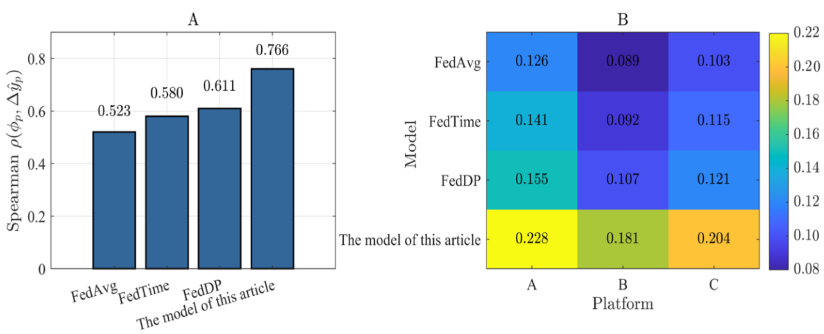

FIGURE 7. Attribution consistency and platform blocking prediction error. Figure 7A: Attribution consistency; Figure 7B: Prediction error

proposed model is generally more ideal in terms of attribution consistency and platform blocking prediction error. As shown in the Spearman's ρ results in Figure 7A, the attribution consistency of the FedAvg, FedTime, and FedDP models is 0.523, 0.580, and 0.611, respectively, while the proposed model reaches 0.766, representing improvements of 46.5%, 32.1%, and 25.4%, respectively. This indicates that the Shapley attribution results output by the model are more strongly correlated with the true counterfactual effect. This demonstrates that, with the synergistic effect of multiple platform touchpoints, the proposed model can more accurately capture the causal contribution of each platform, avoiding the attribution bias caused by information fragmentation in traditional FL models. Regarding the prediction error in Figure 7B, although the proposed model has a slightly higher overall error, reaching 0.228, 0.181, and 0.204 for each platform, respectively, this sensitivity to missing platforms reflects that the model better identifies the causal role of cross-platform touchpoints in the conversion path. In contrast, while FedAvg and FedTime are more robust to platform masking, their attribution consistency is significantly lower, suggesting that their robustness stems from their neglect of causal structure. By combining these two types of indicators, the proposed model can sensitively capture the impact of platform omissions on causal predictions while ensuring attribution rationality.

C. MARKETING OPTIMIZATION

To validate the effectiveness of the proposed system model in actual marketing activities, this article constructs 30 days of simulated experimental data, covering three budget modes: uniform allocation, historical allocation, and optimization strategy, and applies counterfactual inference methods to quantify conversion improvement. By comparing the ROI curve with the trend of conversion numbers, its effectiveness in improving marketing effectiveness and mitigating attribution bias is demonstrated, as shown in Figure 8.

Figure 8 demonstrates that the proposed system achieves relatively promising results in marketing optimization. In Figure 8A, ROI fluctuates over the duration of the campaign. The uniform and historical allocation strategies maintain

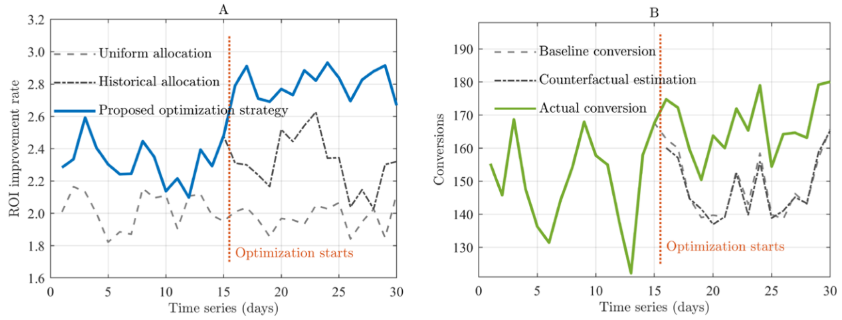

FIGURE 8. ROI and conversion improvement. Figure 8A: ROI comparison of budget optimization strategies; Figure 8B: Conversion improvement based on counterfactual estimation

a low ROI. However, the optimization strategy based on feedback from the proposed evaluation system significantly increases ROI after applying dynamic budget adjustments on day 16, and maintains a high level for subsequent days. The proposed optimization strategy achieves significant improvements compared to both uniform and historical allocation, demonstrating that dynamic budget allocation based on attribution results can effectively maximize marketing return on investment. This mechanism stems from the fact that the system model in this article can identify the contribution of each platform and user group in real time based on attribution results, thereby rationally tilting marketing budget to efficient platforms and high-potential users, achieving optimal resource allocation, and thus improving overall ROI. Figure 8B illustrates the conversion improvement based on counterfactual estimation. Compared to the baseline conversion and counterfactual estimates, the actual conversion number is higher, demonstrating that the optimization strategy informed by this evaluation system can effectively drive changes in user behavior. Leveraging the cross-platform information integration capabilities of the proposed VFL framework, the quantification of contribution through attribution analysis, and the real-time budget adjustment of the proposed dynamic optimization strategy, significant conversion improvements are achieved in actual marketing campaigns, validating the reliability and effectiveness of the proposed optimization strategy in dynamic marketing budget allocation and user conversion improvement.

D. PRIVACY PROTECTION AND COMPLIANCE

In the privacy protection and compliance evaluation section of this article, the advantages of the proposed dynamic cross-platform social media marketing effectiveness evaluation system in protecting user privacy and meeting compliance requirements are validated. By setting different privacy budgets, the information leakage risk and compliance coverage of each model are evaluated. Information leakage risk is measured by the probability of a simulated attack success, while compliance coverage is represented by the pass rate of the system's compliance checks on each platform. The results are shown in Figure 9:

In Figure 9, as the privacy budget increases, the risk decreases, and the compliance coverage increases. In Figure 9A, when the privacy budget is 0.5, the information leakage risk probabilities of the other three models reach 0.382, 0.351, and 0.200, respectively, while that of the proposed model is 0.184, representing reductions of 51.8%, 47.6%, and 8.0%, respectively, compared to the comparison models. In Figure 9B, the compliance coverage of the other three models is lower than that of the proposed model at all privacy budgets. FedDP effectively reduces risk and improves compliance through gradient clipping and DP noise, but still falls slightly short of the proposed model. The FedTime model improves slightly by applying time series features, but still maintains a certain level of leakage risk and struggles to fully meet platform compliance requirements. FedAvg performs the worst, demonstrating that model design alone cannot fully meet privacy and compliance requirements. The proposed method is based on a cross-platform FL framework to achieve collaborative training under the premise of ensuring that data is not shared, and combines causal modeling to improve the accuracy of dynamic evaluation. With the joint application of the DP mechanism and compliance strategy, a more ideal privacy protection and compliance guarantee is formed.

VIII. ANALYSIS OF THE COMPUTATIONAL OVERHEAD INTRODUCED BY THE PRIVACY MECHANISM

To objectively evaluate the impact of privacy mechanisms on system efficiency, this article compares the training and inference times under three configurations in the same hardware environment:

(1) Non-Private VFL: standard vertical federated neural network, without SMPC and DP.

(2) VFL+SMPC: only SMPC based on secret sharing is enabled for secure aggregation of hidden layers.

(3) Full Privacy (the model in this article): SMPC and gradient pruning plus Gaussian noise DP mechanism are enabled simultaneously.

The average training time and single inference latency are recorded in each communication cycle. The results are shown in Table 3.

Table 3 shows that the increase in training time due to

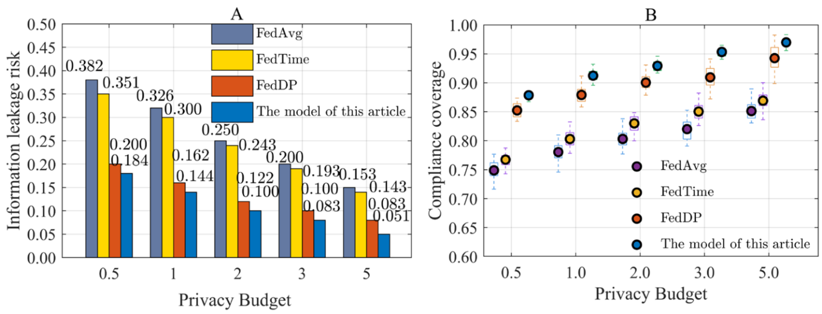

FIGURE 9. Information leakage risk and compliance coverage. Figure 9A: Information leakage risk; Figure 9B: Compliance coverage

TABLE 3. Comparison of computational overhead under different privacy configurations

Specifications	Average Training Time per Round (seconds)	Single Inference Latency (milliseconds)	Communication Volume per Round (MB)
Non-Private VFL	18.3	12.4	0.82
VFL + SMPC	36.7	28.9	1.95
Full Privacy	41.2	31.6	2.03

the introduction of SMPC is mainly due to the additional operations of encrypted fragment generation, cross-platform exchange, and secure aggregation. Further addition of the DP mechanism increases training time again, primarily due to the local computational overhead of gradient pruning and noise injection. During the inference phase, the latency increases from 12.4 ms to 31.6 ms due to the need to perform masked implicit representation upload and coordinator secure reconstruction, and the communication volume also doubles due to SMPC fragment transmission. Despite these overheads, the proposed system still meets the timeliness requirements of real-world marketing scenarios: under the business constraints of daily model updates and second-level online inference, the latency is within an acceptable range. By adopting gradient compression and asynchronous scheduling strategies, the communication burden can be further reduced in subsequent optimizations.

IX. CONCLUSIONS

To address the vulnerability in causal effect identification from heterogeneous cross-platform user behavior and data privacy—challenges particularly acute for the industry's multi-channel marketing strategies—this article constructs a dynamic cross-platform social media marketing effectiveness evaluation system integrated with FL. By building a privacy-coordinated framework based on PSI and VFL, this system securely aligns user identities across multiple platforms and jointly models local features without leaving the domain. A federated attribution mechanism combining Shapley values with counterfactual analysis improves the causal rationality of cross-platform contribution decomposition. In experimental analysis, the model in this article achieves an AUC of 0.897 in terms of predictive performance, with an accuracy of up to 0.876 and an attribution consistency of 0.766. Its marketing optimization effect is superior to the FedAvg, FedTime, and FedDP baseline methods. At the same time, it has a lower risk of information leakage and a higher compliance coverage rate under a low privacy budget. This article provides a reference for cross-platform marketing evaluation in privacy-sensitive scenarios, offering a valuable framework for the global industry to promote the trusted, intelligent application of FL in its complex digital marketing efforts.

AUTHOR CONTRIBUTIONS

Shihua Zuo designed, collected and analyzed the data, and drafted the manuscript. Shihua Zuo conducted the study, critically revised the manuscript for important intellectual content, and gave final approval of the version to be published. Shihua Zuo participated fully in the work, take public responsibility for appropriate portions of the content, and agreed to be accountable for all aspects of the work in ensuring that questions related to the accuracy or integrity of any part of the work are appropriately investigated and resolved.

CONFLICTS OF INTEREST

The author declares no conflict of interest.

FUNDING

This research received no external funding.

ACKNOWLEDGEMENTS

Not applicable.

REFERENCES

[1] H. Heo and S. Lee, "Consumer information-seeking and cross-media campaigns: An interactive marketing perspective on multi-platform strategies and attitudes toward innovative products," Journal of Theoretical and Applied Electronic Commerce Research, vol. 20, no. 2, pp. 68-88, 2025, doi: 10.3390/jtaer20020068.

[2] A. Espinoza and C. A. Pina-Garcia, "(Counter) marketing and misinformation: A cross-platform study," Cogent Business & Management, vol. 11, no. 1, pp. 1-23, 2024, doi: 10.1080/23311975.2024.2398713.

[3] A. Yin, "Research on the Balancing Mechanism between Big Data Precision Marketing and User Privacy Protection," E-Commerce Letters, vol. 14, no. 4, pp. 2015-2019, 2025, doi: 10.12677/ecl.2025.1441101.

[4] J. Liu, "Research on Collaborative Governance of Data Ownership Allocation and Value Distribution on Chinese E-commerce Platforms," E-Commerce Letters, vol. 14, no. 8, pp. 197-204, 2025, doi: 10.12677/ecl.2025.1482509.

[5] O. T. Kufile, B. O. Otokiti, A. Y. Onifade, B. Ogunwale, and C. H. Okolo, "Constructing cross-device ad attribution models for integrated performance measurement," IRE J, vol. 4, no. 12, pp. 460-476, 2021.

[6] K. Mehta and E. Singhal, "Marketing channel attribution modelling: Markov chain analysis," International Journal of Indian Culture and Business Management, vol. 21, no. 1, pp. 63-77, 2020, doi: 10.1504/IJICBM.2020.109344.

[7] X. Liang, "Research on the Dynamic Strategy of Social Media Marketing with AI Enablement–Construction of Interaction Mechanism Based on Sentiment Analysis and Real-time Feedback," Journal of Technology Innovation and Engineering, vol. 1, no. 1, pp. 1-10, 2025, [Online]. Available: https://www.sci-open.net/index.php/JTIE/article/view/498.

[8] J. Liu, W. Zhong, J. Zhang, and S. E. Mei, "The effectiveness of cross-platform targeted advertising strategy," Electronic Commerce Research, vol. 24, no. 4, pp. 2831-2847, 2024, doi: 10.1007/s10660-022-09659-0.

[9] O. T. Kufile, O. V. Akinrinoye, A. Y. Onifade, O. G. Ejike, B. O. Otokiti, and S. A. Umezurike, "Developing conceptual attribution models for cross-platform marketing performance evaluation," International Journal of Multidisciplinary Research and Growth Evaluation, vol. 4, no. 2, pp. 844-854, 2023, doi: 10.54660/.IJMRGE.2023.4.2.844-854.

[10] G. Kou, P. Yang, Y. Peng, H. Xiao, F. Xiao, Y. Chen, et al., "A cross-platform market structure analysis method using online product reviews," Technological and Economic Development of Economy, vol. 27, no. 5, pp. 992-1018, 2021, doi: 10.3846/tede.2021.12005.

[11] H. Krijestorac, R. Garg, and V. Mahajan, "Cross-platform spillover effects in consumption of viral content: A quasi-experimental analysis using synthetic controls," Information Systems Research, vol. 31, no. 2, pp. 449-472, 2020, doi: 10.1287/isre.2019.0897.

[12] M. Poturak and D. Durakovic, "Evaluating the effectiveness of social media advertising strategies across different demographics and platforms," International Journal of Research in Business & Social Science, vol. 14, no. 6, pp. 10-29, 2025, doi: 10.20525/ijrbs.v14i6.4341.

[13] M. Kaveh, S. Saeida Ardekani, and S. M. Tabatabaeenasab, "Marketing Strategy Evaluation by Integrating Dynamic Systems Modeling and Network Data Envelopment Analysis," Journal of System Management, vol. 2, no. 1, pp. 19-34. https://doi.org/10.30495/JSM.2020.673643, 2020.

[14] K. Zhang and P. Li, "Federated learning optimizing multi-scenario ad targeting and investment returns in digital advertising," Journal of Advanced Computing Systems, vol. 4, no. 8, pp. 36-43, 2024, doi: 10.69987/JACS.2024.40806.

[15] W. Ali, X. Zhou, and J. Shao, "Privacy-preserved and responsible recommenders: From conventional defense to federated learning and blockchain," ACM Computing Surveys, vol. 57, no. 5, pp. 1-35, 2025, doi: 10.1145/3708982.

[16] K. Zhang, S. Xing, and Y. Chen, "Research on Cross-Platform Digital Advertising User Behavior Analysis Framework Based on Federated Learning," Artificial Intelligence and Machine Learning Review, vol. 5, no. 3, pp. 41-54, 2024, doi: 10.69987/AIMLR.2024.50304.

[17] X. Zhang and C. Guo, "Research on Open Innovation Intelligent Decision-Making of Cross-Border E-Commerce Based on Federated Learning," Mathematical Problems in Engineering, vol. 2022, no. 1, pp. 1-13, 2022, doi: 10.1155/2022/9253634.

[18] D. Kim, H. Woo, and Y. Lee, "Addressing bias and fairness using fair federated learning: A synthetic review," Electronics, vol. 13, no. 23, pp. 4664-4669, 2024, doi: 10.3390/electronics13234664.

[19] Y. Liang, J. Ma, Y. Miao, D. Kuang, X. Meng, and R. H. Deng, "Privacy-preserving bloom filter-based keyword search over large encrypted cloud data," IEEE Transactions on Computers, vol. 72, no. 11, pp. 3086-3098, 2023, doi: 10.1109/TC.2023.3285103.

[20] Z. Jin, D. Li, X. Zhang, and Z. Cai, "Research on dynamic searchable encryption method based on Bloom filter," Applied Sciences, vol. 14, no. 8, pp. 3379-3402, 2024, doi: 10.3390/app14083379.

[21] F. Koltuk and E. G. Schmidt, "Uniformity and independence of H3 hash functions for Bloom filters," IEEE Transactions on Computers, vol. 73, no. 8, pp. 1913-1923, 2024, doi: 10.1109/TC.2024.3398426.

[22] L. Lyu, H. Yu, X. Ma, C. Chen, L. Sun, J. Zhao, et al., "Privacy and robustness in federated learning: Attacks and defenses," IEEE Transactions on Neural Networks and Learning Systems, vol. 35, no. 7, pp. 8726-8746, 2022, doi: 10.1109/TNNLS.2022.3216981.

[23] Y. Liu, Y. Kang, T. Zou, Y. Pu, Y. He, X. Ye, et al., "Vertical federated learning: Concepts, advances, and challenges," IEEE Transactions on Knowledge and Data Engineering, vol. 36, no. 7, pp. 3615-3634, 2024, doi: 10.1109/TKDE.2024.3352628.

[24] M. Ye, W. Shen, B. Du, E. Snezhko, V. Kovalev, and P. C. Yuen, "Vertical federated learning for effectiveness, security, applicability: A survey," ACM Computing Surveys, vol. 57, no. 9, pp. 1-32, 2025, doi: 10.1145/3720539.

[25] D. Cai, T. Fan, Y. Kang, L. Fan, M. Xu, S. Wang, et al., "Accelerating vertical federated learning," IEEE Transactions on Big Data, vol. 10, no. 6, pp. 752-760, 2022, doi: 10.1109/TBDATA.2022.3192898.

[26] J. Zhang, S. Guo, Z. Qu, D. Zeng, H. Wang, Q. Liu, et al., "Adaptive vertical federated learning on unbalanced features," IEEE Transactions on Parallel and Distributed Systems, vol. 33, no. 12, pp. 4006-4018, 2022, doi: 10.1109/TPDS.2022.3178443.

[27] Z. Wu, Q. Li, and B. He, "Practical vertical federated learning with unsupervised representation learning," IEEE Transactions on Big Data, vol. 10, no. 6, pp. 864-878, 2022, doi: 10.1109/TBDATA.2022.3180117.

[28] D. Gao, D. Chen, Z. Li, Y. Xie, X. Pan, Y. Li, et al., "Fs-real: A real-world cross-device federated learning platform," Proceedings of the VLDB Endowment; 28 August-01 September 2023; Vancouver, Canada. Los Angeles, CA, USA: VLDB Endowment; 2023; 16(12):4046-4049, doi: 10.14778/3611540.3611617.

[29] P. C. Hong, Y. S. Park, X. Deng, and D. W. Hwang, "Marketing platform products for successful customer outcomes: An empirical investigation of project process integration," International Journal of Quality and Service Sciences, vol. 14, no. 3, pp. 349-367, 2022, doi: 10.1108/IJQSS-09-2021-0130.

[30] Hair Jr, F. Joseph, and M. Sarstedt, "Data, measurement, and causal inferences in machine learning: Opportunities and challenges for marketing," Journal of Marketing Theory and Practice, vol. 29, no. 1, pp. 65-77. https://doi.org/10.1080/10696679.2020.1860683, 2021.

[31] D. P. Uddandarao, "Measuring Negative Causal Impact of Product Launches Using Constrained Shapley-based Causal Inference," Journal of Computational Analysis & Applications, vol. 34, no. 5, pp. 201-209. https://doi.org/10.48047/jocaaa.2025.34.05.15, 2025.

[32] R. Sura, "The Role of Causal Inference in Business Decision-Making and A/B Testing at Scale," ESP Journal of Engineering & Technology Advancements, vol. 5, no. 2, pp. 96-103. https://doi.org/10.56472/25832646/JETA-V5I2P111, 2025.

[33] B. R. Chadagonda, "Optimizing Marketing Spend with Causal Attribution: Moving Beyond Correlation to Incremental Impact," Journal Of Engineering and Computer Sciences, vol. 4, no. 8, pp. 150-157, 2025, doi: 10.5281/zenodo.16754685.

[34] D. Patel, "Optimizing Digital Marketing Through Cross-Platform Data Integration: A Focus on Facebook Campaign Efficiency," Scientific Research Journal of Science, Engineering and Technology, vol. 1, no. 2, pp. 22-25, 2023, [Online]. Available: https://isrdo.org/journal/SRJSET/currentissue/optimizing-digital-marketing-through-cross-platform-data-integration-a-focus-on-facebook-campaign-efficiency.

[35] Y. Jia, H. Feng, X. Wang, and M. Alvarado, ""Customer reviews or vlogger reviews?" The impact of cross-platform ugc on the sales of experiential products on E-commerce platforms," Journal of Theoretical and Applied Electronic Commerce Research, vol. 18, no. 3, pp. 1257-1282, 2023, doi: 10.3390/jtaer18030064.

[36] J. Su, X. Luo, H. Li, and H. Xiao, "Unlocking the Power of User Tie Strength: A Multistudy on Cross-Platform Content Sharing Behaviors," Journal of the Association for Information Systems, vol. 26, no. 5, pp. 1457-1484, 2025, doi: 10.17705/1jais.00942.